

## SCATTERING STUDIES ON POLYMER COLLOIDS UNDER SHEAR

R. H. OTTEWILL<sup>1</sup> and A. R. RENNIE<sup>2</sup>

<sup>1</sup>School of Chemistry, University of Bristol, Cantock's Close, Bristol BS8 1TS, England

<sup>2</sup>Institut Laue-Langevin, Grenoble, France

(Received 4 June 1989; in revised form 15 February 1990)

**Abstract**—Neutron beams are easily transmitted through optically opaque samples and therefore provide an excellent means of examining concentrated colloidal dispersions. Small-angle neutron scattering studies can, moreover, provide a means of determining the structure of such systems both in an equilibrium mode and under dynamic conditions. The present investigation is concerned with the latter and describes the examination of two types of colloidal dispersion in a quartz Couette viscometer at shear rates up to  $10,000 \text{ s}^{-1}$ . In the case of an aqueous dispersion of monodisperse charged polystyrene particles the system under static conditions was quasi-crystalline but “melted” under the influence of the shear field. With sterically stabilized dispersions of poly(methyl methacrylate) particles in dodecane it was found that under shear different structural arrangements of the particles occurred in directions perpendicular and parallel to the direction of flow.

*Key Words:* polymer colloids, neutron scattering, sheared systems, ordered structures.

### INTRODUCTION

Rheology is concerned with the flow and deformation of materials (Reiner 1960) and most of the instrumentation used for studies in this field essentially measures bulk properties. Consequently, it seems highly desirable to have techniques which can also measure the microstructure of systems under the same conditions as those used for rheological examination. Scattering techniques provide exactly the means to do this and a number of studies have been reported using optical methods (Hoffmann 1972, 1974; van de Ven 1988, 1990; Tomita & van de Ven 1984; Ackerson & Clark 1983, 1984) and also a few using small-angle neutron scattering (Ackerson *et al.* 1986; Lindner *et al.* 1988; Rennie *et al.* 1990; Ashdown *et al.* 1990). In this contribution we present studies using small-angle neutron scattering on both aqueous dispersions of charged polystyrene particles and nonaqueous dispersions of polymethyl methacrylate stabilized by poly(12-hydroxy stearic acid).

Small-angle neutron scattering is an excellent tool for such investigations in that it probes distance scales in the range from 10 to several thousand angstroms. The contrast between particles and medium is such that with neutrons good signals can be obtained and measurements can be made on samples of the order of 1 mm in thickness, even with concentrated dispersions which are opaque to light. Moreover, many materials are transparent to neutrons and hence a wide range of materials are available for the construction of containers to simulate conditions in rheometers.

### THEORY

#### *Small-angle neutron scattering—time average*

For a neutron beam of wavelength,  $\lambda$ , the magnitude of the scattering vector for elastic scattering is given by

$$\mathbf{Q} = 4\pi \sin\left(\frac{\theta}{2}\right) \frac{1}{\lambda}, \quad [1]$$

where  $\theta$  is the scattering angle, i.e. the angle between the incident beam and the scattered radiation. For an ensemble of noninteracting particles, the intensity of the scattered radiation at a scattering

vector  $\mathbf{Q}$  is given by

$$I(\mathbf{Q}) = AN_p V_p^2 (\rho_p - \rho_m)^2 P(\mathbf{Q}), \quad [2]$$

where  $A$  is an instrumental calibration factor,  $V_p$  is the volume of each spherical particle and  $N_p$  is the number of particles per unit volume of the dispersion;  $\rho_p$  is the coherent neutron scattering density of the particle and  $\rho_m$  that of the dispersion medium. For a spherical particle with  $V_p = 4\pi R^3/3$  and  $R$  = particle radius, the volume fraction  $\phi$  is given by  $N_p V_p$ .  $P(\mathbf{Q})$  is the particle shape factor, which is given by

$$P(\mathbf{Q}) = \left[ \frac{3(\sin \mathbf{Q}R - \mathbf{Q}R \cos \mathbf{Q}R)}{(\mathbf{Q}R)^3} \right]^2. \quad [3]$$

In practice, allowance can be made for polydispersity and the technique used to determine particle size distributions (Ottewill 1987).

In dispersions where the particles are interacting, however, the particles are unable to diffuse unhindered and the interactions produce correlations between the particle positions. Hence a degree of order is imparted to the dispersion, which depends on the volume fraction and the strength of the repulsive interactions: for scattering experiments on such systems the interference of the radiation scattered by the correlated particles has to be taken into account and leads to an expression for intensity in the form

$$I(\mathbf{Q}) = I(\mathbf{Q})_{\text{part}} S(\mathbf{Q}), \quad [4]$$

where  $I(\mathbf{Q})_{\text{part}}$  is the intensity of scattering from noninteracting particles (cf. [2]) and the term  $S(\mathbf{Q})$  is called the structure factor. This can be written in the form

$$S(\mathbf{Q}) = 1 + \frac{4\pi N_p}{\mathbf{Q}} \int_0^\infty [g(r) - 1] r \sin \mathbf{Q}r \, dr, \quad [5]$$

where  $r$  = the centre-to-centre distance between the particles and  $g(r)$  = the particle-pair distribution function.

For an interacting system of spherical particles measured under static conditions the scattered intensity is

$$I(\mathbf{Q}) = [A(\rho_p - \rho_m)^2 V_p \phi P(\mathbf{Q})] S(\mathbf{Q}). \quad [6]$$

Since the term in square brackets can be obtained from an experiment on a dilute dispersion,  $S(\mathbf{Q})$  as a function of  $\mathbf{Q}$  can be obtained from the experimental  $I(\mathbf{Q})$  vs  $\mathbf{Q}$  data on a concentrated system. Previous investigations have used this procedure for both aqueous and nonaqueous polymer lattices (Ottewill 1989).

For dispersions undergoing shear it seems reasonable to assume that for rigid polymer latex particles, no deformation of the particles will occur even at high shear rates, and thus  $P(\mathbf{Q})$  will be the same at both low and high shear rates. Thus, the changes of  $I(\mathbf{Q})$  vs  $\mathbf{Q}$  which occur in sheared systems can be interpreted as changes in the structure factor  $S(\mathbf{Q})$ , and hence in  $g(r)$ , i.e. changes will occur in the probability of finding neighbouring particles at a given distance and orientation (Ackerson *et al.* 1986; Schwarzl & Hess 1986).

#### *Dynamic effects*

Colloidal particles are in continuous motion as a consequence of continual interaction with solvent molecules, Brownian motion. The extent of this motion is encompassed in the translational diffusion coefficient,  $D$ , which for dilute dispersions is given by the Einstein equation in the form

$$D_0 = \frac{kT}{6\pi\eta R} = \frac{\langle \Delta r(t)^2 \rangle}{6t}, \quad [7]$$

where  $k$  = Boltzmann constant,  $T$  = absolute temperature,  $\eta$  = viscosity and  $\langle \Delta r(t)^2 \rangle$  is the mean square displacement in a time  $t$ . An estimate of the time scale of particle movement can be obtained by using [7] to estimate the time for an unhindered particle in water to diffuse one particle radius. This is shown in table 1.

Table 1. Time scales for diffusion

Particle radius ( $\text{\AA}$ )	$D_0(\text{cm}^2 \text{s}^{-1})$	$t(\mu\text{s})$	$Q(\text{\AA}^{-1})$
100	$2.18 \times 10^{-7}$	$\sim 1$	0.063
500	$4.35 \times 10^{-8}$	$\sim 10^2$	0.013
1000	$2.18 \times 10^{-8}$	$\sim 10^3$	0.006
5000	$4.35 \times 10^{-9}$	$\sim 10^5$	0.001

The small-angle neutron scattering technique provides a spatial probe for investigating distances in real space of the order of  $2\pi/Q$ ; alternatively, it can be regarded as providing the  $Q$  needed to probe one radius, as being of the order of  $2\pi/R$  (see table 1). The instrumental range of  $Q$  available is typically between 0.001 and 0.1  $\text{\AA}^{-1}$  and hence the scale of distance probed can be between ca. 10 and 5000  $\text{\AA}$ .

Investigations of colloid particle dynamics involve the need to probe dispersions over a range of scattering vectors and time scales. This is illustrated schematically in figure 1 to show the techniques which are available by using scattering measurements. In particular, this illustrates that by the use of a shear flow, small-angle scattering can access scattering vectors between 0.001 and 0.1  $\text{\AA}^{-1}$  and time scales between ca. 0.1 ms and 1 s by using shear rates between 1 and  $10^4 \text{s}^{-1}$ . Since time scale is important we can estimate approximately from table 1 that a 100  $\text{\AA}$  radius particle will need high rates of shear (ca.  $10^6 \text{s}^{-1}$ ) to damp out the Brownian motion, whereas particles of radius 1000  $\text{\AA}$  should be damped at shear rates of the order of  $10^3 \text{s}^{-1}$ . For this reason we selected dispersions for examination which contained particles of dia ca. 0.2  $\mu\text{m}$ .

## EXPERIMENTAL

### *Aqueous latex*

This was a polystyrene latex (SP12) in water, whose preparation has been described previously (Goodwin *et al.* 1974). It was deionized by treatment with mixed bed ion-exchange resin; the latter was treated in the manner described by van den Hul & Vanderhoff (1970). The number average

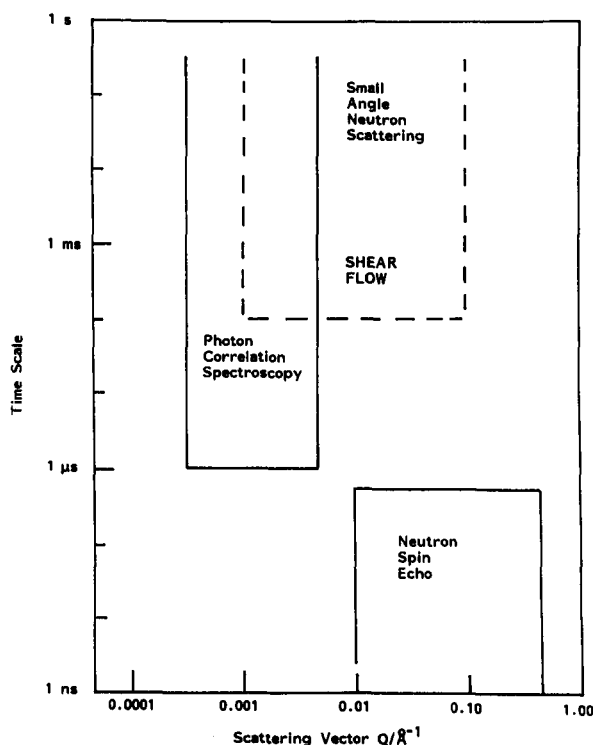


Figure 1. Schematic illustrations showing the regions of time and the scattering vector which can be utilized to investigate the dynamics of colloidal particles.

diameter of the particles, determined by electron microscopy, was 2050 Å with a coefficient of variation on the mean diameter of 7%.

#### *Nonaqueous latex*

The particles were composed of a spherical core of poly(methyl methacrylate) stabilized by an outer layer of poly(12-hydroxy stearic acid); the latter was chemically grafted to the core particle using the synthesis described previously (Antl *et al.* 1986). The number average diameter was 2080 Å with a coefficient of variation of 10%.

#### *Small-angle neutron scattering*

Experiments were carried out using the neutron diffractometer D11 at the Institut Laue-Langevin, Grenoble, France (ILL 1988). This instrument is equipped with a two-dimensional position-sensitive detector, with a square matrix of  $64 \times 64$  detector elements (4096 in total) each with an area of  $1 \text{ cm}^2$ . This allowed two-dimensional contour plots to be obtained showing lines of equal intensity or three-dimensional plots showing intensity across the detector. The detector was movable but for the experiments described was located at 35.7 m from the sample. A neutron beam of wavelength 9.96 Å was used with a  $\Delta\lambda/\lambda$  of 10%. The incident beam was collimated with simple apertures to provide a beam of cross-section  $1 \text{ cm}^2$  on the sample. The incoherent backgrounds from the samples were found to be negligible in comparison with the coherent intensity in the diffraction peaks. The neutron counts in the 4096 detector cells were stored on magnetic tape and used for either isotropic or anisotropic analysis according to the conditions used.

#### *Couette viscometer*

All the latex samples were examined in a quartz Couette shear cell of the type described by Lindner & Oberthür (1984) and also used in our previous work (Lindner *et al.* 1988; Rennie *et al.* 1990; Ashdown *et al.* 1990). The cell was fitted with a variable-speed motor, so that by using a gap width of 0.5 mm it was possible to make measurements over a range of shear rates from ca.  $10$  to  $10^4 \text{ s}^{-1}$ ; measurements could also be made with this system under static conditions. The cell produced a uniform shear gradient in the direction of the incident neutron beam, as shown in figure 2. It should be noted that the beam passed through the cell twice; however, since the overall diameter of the cell was ca. 5 cm and the sample-detector distance was 35.7 m, any deviation caused by this arrangement was not observable experimentally. The intensity patterns displayed on the planar detector were in a direction normal to the shear gradient. Hence, the horizontal display on the detector gave information in a direction parallel to that of the flow and in a direction perpendicular to the direction of flow, as shown in figure 2. The cell was thermostatted at  $25^\circ\text{C}$  during measurements.

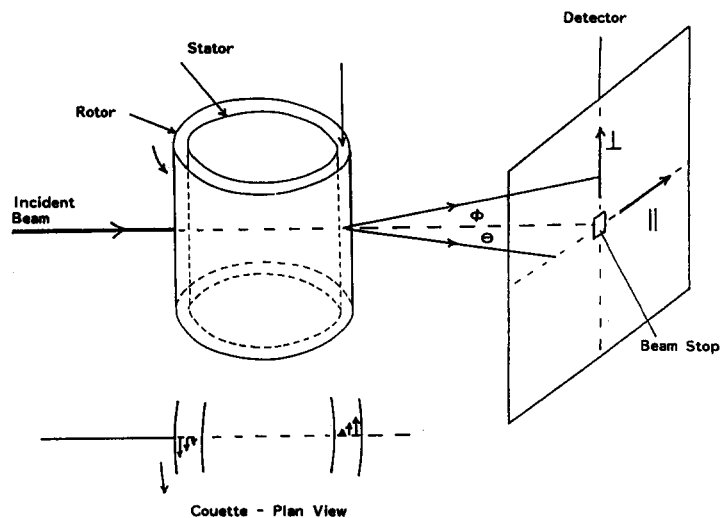


Figure 2. Schematic illustration of the quartz Couette cell used for scattering measurements on sheared systems.

## RESULTS AND DISCUSSION

*Aqueous polystyrene latices*

Figure 3 shows a series of neutron diffraction patterns obtained in the shear cell on an aqueous ion-exchange treated sample of the latex SP12 at a volume fraction of 0.087. The figures are presented in the form of two-dimensional contour displays of lines of equal intensity, namely  $I(\mathbf{Q})$ . The rectangular section in the centre of the pattern is that of the cadmium beam-stop profile; the latter is placed just before the detector to protect it from the primary beam. The size of the spots in the pattern is to a large extent controlled by the size of the apertures placed before the collimator section and the cell.

The pattern shown in figure 3(a) was obtained under static conditions. Since it was observed with a wide beam, in transmission, the clarity of the spot pattern implies that there are large spatial domains within the sample which are "crystalline" in nature. Within the limits of experimental accuracy good correspondence was found between the observed spots and the calculated spot positions for an f.c.c. lattice oriented with a (111) face against the surface of the Couette cell. The spacings correspond to a unit cell dimension of 6400 Å.

At a shear rate of  $10 \text{ s}^{-1}$  [figure 3(b)] there is a loss of intensity in the outer spots and this becomes even more pronounced at a shear rate of  $1600 \text{ s}^{-1}$  [figure 3(c)]; at both shear rates, however, the essentially crystalline configuration is retained. At  $6400 \text{ s}^{-1}$  the outer spots have essentially disappeared, although the inner hexagonal array at low  $\mathbf{Q}$  values still remains very pronounced [figure 3(d)]. At  $10^4 \text{ s}^{-1}$  the four inner spots are still clearly visible but there is considerably less structure at the higher  $\mathbf{Q}$  values [figure 3(e)]. In all the sheared systems there appears to be a more clearly defined pattern in the direction perpendicular to that of the flow than in the direction parallel to the flow.

In figure 4 an illustration is given of  $I(\mathbf{Q})$  vs  $\mathbf{Q}$  for a line of detector cells taken through the centre of the detector. At zero rate of shear there is an intense peak at  $\mathbf{Q} = 0.0027 \text{ \AA}^{-1}$  which corresponds to a (022) reflection. This peak is still clearly visible at  $1600 \text{ s}^{-1}$  but a new peak has appeared at

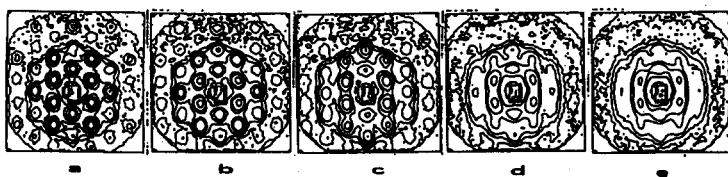


Figure 3. Contour plots of constant intensity,  $I(\mathbf{Q})$ , plotted vs  $\mathbf{Q}$ , obtained in measurements on ion-exchanged latex SP12, volume fraction 0.087, at various rates of shear: (a) 0; (b)  $10 \text{ s}^{-1}$ ; (c)  $1600 \text{ s}^{-1}$ ; (d)  $6400 \text{ s}^{-1}$ ; (e)  $10,000 \text{ s}^{-1}$ .

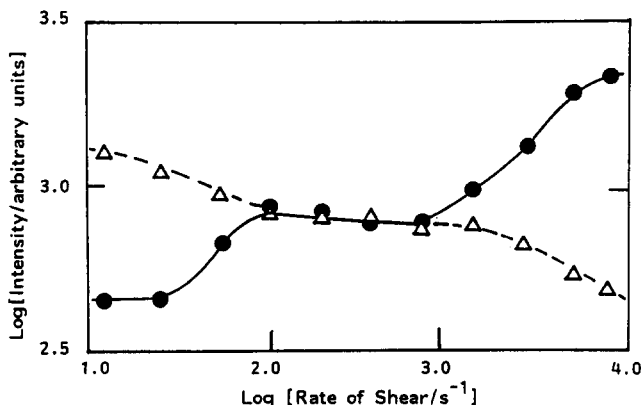


Figure 5.  $\text{Log } I(\mathbf{Q})$  vs  $\text{log}$  shear rate for ion-exchanged latex SP12, at a volume fraction of 0.087, for (111) reflections (●) and (022) reflections (△).

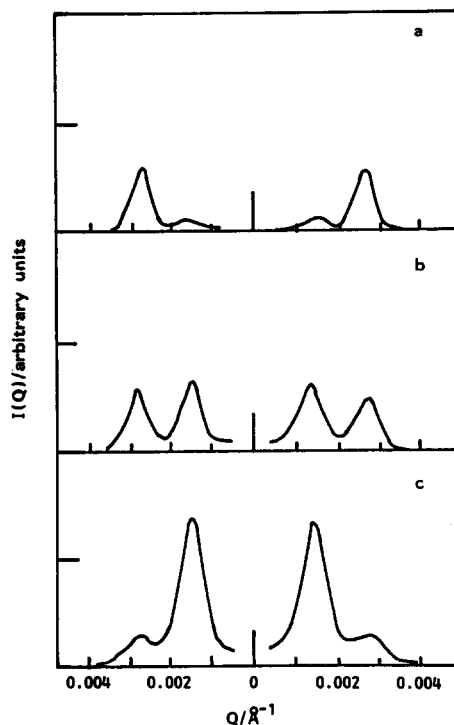


Figure 4. Intensity,  $I(\mathbf{Q})$ , vs  $\mathbf{Q}$  for a line across the detector horizontally through the centre position, i.e. in the direction of flow, at various rates of shear for ion-exchanged latex SP12, volume fraction 0.087: (a) 0; (b)  $1600 \text{ s}^{-1}$ ; (c)  $10,000 \text{ s}^{-1}$ .

$Q = 0.0014 \text{ \AA}^{-1}$ . A further increase of shear rate to  $10^4 \text{ s}^{-1}$  increases the intensity of the first peak quite considerably but the second is reduced and moves to a higher  $Q$  value; the form of the curve now clearly resembles those obtained in an examination of systems having a liquid-like structure, i.e. a pronounced peak in  $S(Q)$  at low  $Q$  values with peaks of diminishing amplitude at higher  $Q$  values—indicating short-range order but long-range disorder (Ottewill 1989).

An alternative method of examining the data is to consider the radial average of intensity taken in a narrow sector in a given direction. The results obtained based on a  $15^\circ$  sector are shown in figure 5 for the (111) and (022) reflections as a function of shear rate parallel to the direction of the flow. The (111) reflection increases in intensity between 10 and  $100 \text{ s}^{-1}$ , remains nearly constant between 100 and  $1000 \text{ s}^{-1}$  and then increases rapidly between 1000 and  $10,000 \text{ s}^{-1}$ . On the other hand, over the same shear rate changes, the (022) reflection decreases, remains nearly constant and then decreases further. A possible interpretation of these results is that at rest, although the system is essentially crystalline, there is still space for the particles to undergo self-diffusion, thus weakening the order in the (111) planes. On applying the shear this diffusion is overcome by the shearing motion, the planes become more ordered and the intensity of reflection for this spacing is increased. The (022) planes are less densely packed initially and, on shearing, the particles in these planes become more firmly integrated into the (111) planes. It can thus be tentatively inferred from these data that at shear rates up to ca.  $1600 \text{ s}^{-1}$  the particles tend to form close-packed planes which rotate concentrically in the form of a distorted hexagonally packed arrangement. The distortion of the hexagonal pattern indicates that under shear the particles are more spread out in the direction of flow and move closer together in the vertical direction. This might arise as a consequence of the distortion of the electrical double layer, which, instead of being spherically symmetrical as at rest, would become distorted in the direction of flow, thus increasing repulsion along the direction of the flow lines whilst allowing closer approach in the direction perpendicular to flow.

At high shear rates the high-order diffraction spots disappear. This appears to be associated with shear-induced melting of the lattice with the energy for the melting process being supplied by the shear field. It should be emphasized, as discussed elsewhere (Ashdown *et al.* 1990), that crystalline samples are not always obtained on filling the cell. Frequently, however, they can be organized by applying a shear field to the system (Ashdown *et al.* 1990).

#### *Nonaqueous dispersions*

A number of measurements have been made on sterically stabilized particles, composed of a core of poly(methyl methacrylate) with a stabilizing layer of poly(12-hydroxy stearic acid), in dodecane. As an example, we report here the results obtained from an examination of a 44% w/w (volume fraction ca. 0.40) sample SPSO90 in the form of contour plots of equal intensity,  $I(Q)$ , at zero shear, 300, 1000 and  $6000 \text{ s}^{-1}$  (figure 6). It can be seen from the contours that a zero shear rate there is a centro-symmetric peak in intensity which arises from the first maximum in a liquid-like system (Marković *et al.* 1986). A number of changes that occur under sheared conditions are observable from the patterns. Firstly, as the shear rate is increased the intensity at low  $Q$  increases in the direction of the detector parallel to the direction of flow in the Couette viscometer. Secondly, in the direction on the detector perpendicular to the direction of flow a clearly defined peak remains and this moves to high  $Q$  values as the rate of shear is increased.

These changes can also be clearly seen by taking  $I(Q)$  vs  $Q$  sections across the detector: in order to do this the data in sectors, on the detector, in the direction of flow (horizontal direction in figure 6), as  $0^\circ \pm 15^\circ$ , and perpendicular to flow,  $90^\circ \pm 5^\circ$ , were taken and radially averaged over the  $30^\circ$  sector. The results are illustrated in figures 7(a–c); in all these figures the curve at zero shear rate is plotted as the reference curve. In figure 7(a), in the direction of flow, at  $300 \text{ s}^{-1}$  the peak has moved to a lower  $Q$  value and at  $10,000 \text{ s}^{-1}$  the peak has either disappeared or moved to a much lower  $Q$  value—indicating a lack of correlation between the particles. Since, as shown in [6], the changes in  $I(Q)$  are essentially reflecting changes in the structure factor; these results could suggest that structure is being lost under shear in the direction of flow with the system behaving as though it were becoming more dilute so that the frequency of particle–particle interactions was reduced. On the other hand, in the direction perpendicular to the direction of flow [figure 7(b)], the intensity is reduced and the peak moves to a high  $Q$  value. This implies that the structure factor,  $S(Q)$ , is

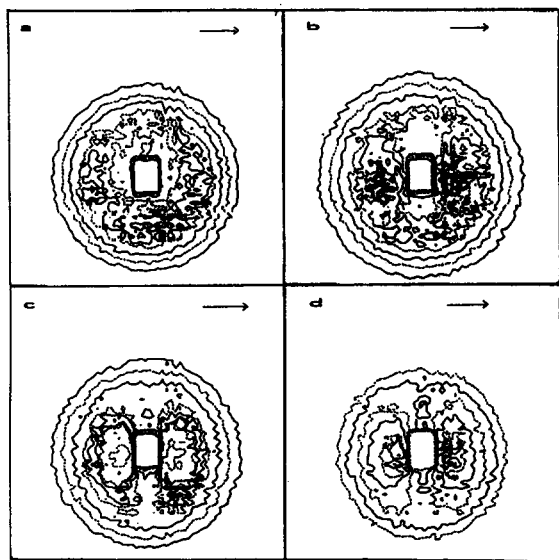


Figure 6. Contour plots of constant intensity,  $I(Q)$ , plotted vs  $Q$  for a PMMA-PMS latex in dodecane at a concentration of 44% w/w at various shear rates: (a) 0; (b)  $300 \text{ s}^{-1}$ ; (c)  $3000 \text{ s}^{-1}$ ; (d)  $6000 \text{ s}^{-1}$ . The arrow indicates the direction of flow in the Couette cell.

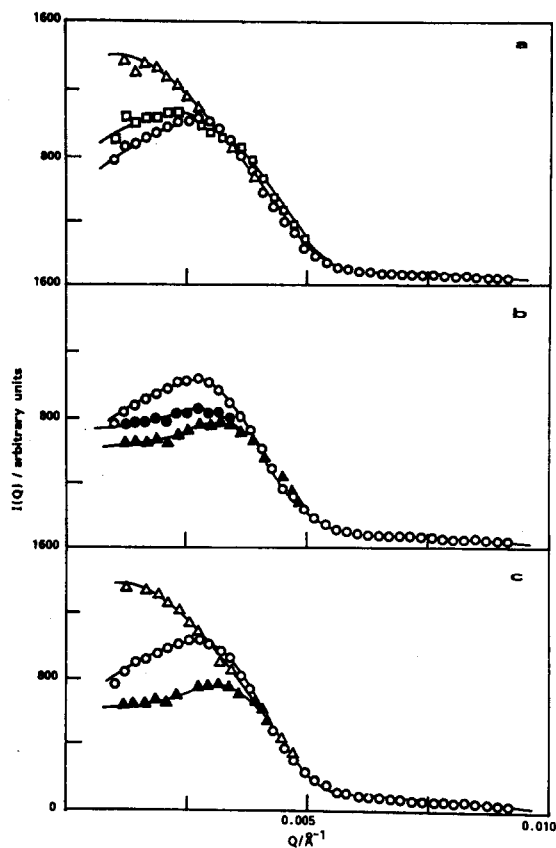


Figure 7.  $I(Q)$  vs  $Q$  for a 44% w/w PMMA-PMS latex in dodecane to illustrate the changes occurring under sheared conditions,  $\circ-\circ$  show measurements under static conditions at zero rate of shear. (a) Measurements parallel to the direction of flow;  $\square$ ,  $300 \text{ s}^{-1}$ ;  $\triangle$ ,  $10,000 \text{ s}^{-1}$ . (b) Measurements perpendicular to the direction of flow:  $\bullet$ ,  $3000 \text{ s}^{-1}$ ;  $\blacktriangle$ ,  $10,000 \text{ s}^{-1}$ . (c) Parallel to the direction of flow— $\triangle$ ,  $10,000 \text{ s}^{-1}$ ; perpendicular to the direction of flow— $\blacktriangle$ ,  $10,000 \text{ s}^{-1}$ .

undergoing changes in the direction of stronger interactions between the particles—an inference that the system is becoming more concentrated and hence more structured. The difference between the two directions is clearly illustrated in figure 7(c) which comprises the results in the perpendicular and parallel directions with those of the static system. A schematic, and probably very approximate, illustration of the particle arrangement is shown in figure 8. At rest the system has a liquid-like structure and then under shear becomes more concentrated in the direction perpendicular to flow. The bulk viscosity of the system plotted against the rate of shear is shown in figure 9. The measurements were made in a Bohlin viscometer (by courtesy of Dr Th. Tadros) and with this

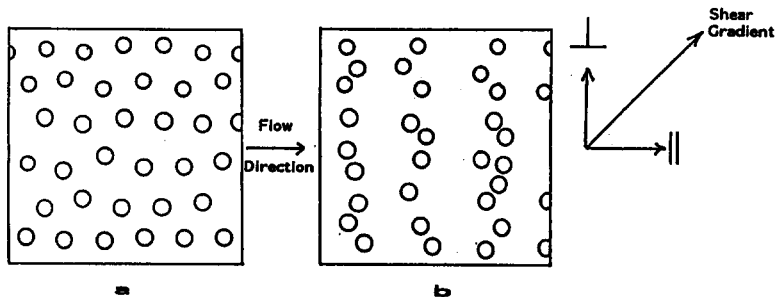


Figure 8. Schematic diagram to illustrate qualitatively the changes in particle-particle arrangement on going from (a) static to (b) sheared conditions.

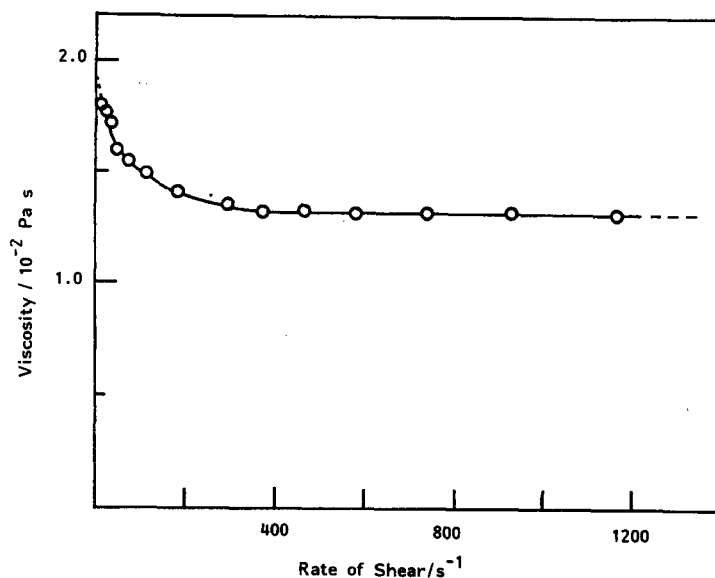


Figure 9. Viscosity vs rate of shear for a PMMA-PMS latex SPSO90 in dodecane at a concentration of 44% w/w.

instrument it was not possible to go beyond a shear rate of  $1170 \text{ s}^{-1}$ . The system shows initially pseudo-plastic behaviour and then becomes essentially Newtonian beyond ca.  $400 \text{ s}^{-1}$ . It is of interest that the small-angle neutron scattering technique was detecting changes in the structure of the system in regions where the viscosity was apparently not changing appreciably, as determined by measurements on the bulk system.

## CONCLUSIONS

The two systems examined, a deionized polystyrene latex in water and a sterically stabilized poly(methyl methacrylate) latex in dodecane, contained particles which were essentially identical in particle size. The observed behaviour of the two systems under shear is quite different. In the aqueous system the strong long-range electrostatic forces between the particles lead to the formation of a highly organized "crystalline" system at a volume fraction of 0.087; this is quite resistant to shearing forces at low shear values but eventually melts at high shear rates. The implication is that at zero shear rates the particles are in deep potential wells and that long-time self-diffusion has essentially ceased. Thus, in order to flow, the system appears to move into hexagonally packed planes which move along parallel flow lines. At very high shear rates enough energy is imparted by shear to cause some "melting" of this arrangement.

In the nonaqueous system the interaction between the particles is close to that of a hard sphere and at a concentration of 44% w/w there is still long-time self-diffusion occurring in the system (Ottewill & Williams 1987; van Meegen *et al.* 1987). The system is also well below the volume fraction of 0.54 predicted by Hoover & Ree (1968) for the onset of freezing in a hard-sphere system. Thus, the system initially has a liquid-like structure with particle-particle interaction occurring by short-range forces but with enough free volume in the system for particle rearrangement to occur. Thus, under shear, considerable particle rearrangement can occur in the manner described with particles moving further apart in the flow direction and apparently forming clusters of particles in the perpendicular direction.

Recently, computer simulation studies have managed to give results in the form observed on the two-dimensional detector in these studies (Hess *et al.* 1989; Loose & Hess 1989). Some close parallels between experiment and theory are observable. Further analysis of the data in terms of current theories, e.g. Ronis (1984, 1986), will be described in later publications.



*Dedication*—One of us (R. H. O.) knew Stan Mason over a period of many years and followed with great admiration his elegant scientific contributions to the field of colloid science and, in particular, the area of microrheology. We regard it as a great privilege to be invited to contribute to his memory in this issue.

*Acknowledgements*—We wish to thank SERC for support of this work and the Institut Laue-Langevin for neutron facilities.

## REFERENCES

- ACKERSON, B. J. & CLARK, N. A. 1983 Sheared colloidal suspensions. *Physica* **118a**, 221–249.
- ACKERSON, B. J. & CLARK, N. A. 1984 Shear-induced partial translational ordering of a colloidal solid. *Phys. Rev.* **A30**, 906–918.
- ACKERSON, B. J., HAYTER, J. B., CLARK, N. A. & COTTER, L. 1986 Neutron scattering from charge stabilized suspensions undergoing shear. *J. chem. Phys.* **84**, 2344–2349.
- ANTL, L., GOODWIN, J. W., HILL, R. D., OTTEWILL, R. H., OWENS, S. M. & PAPWORTH, S. 1986 The preparation of poly(methyl methacrylate) latices in nonaqueous media. *Colloids Surf.* **17**, 67–78.
- ASHDOWN, S., MARKOVIĆ, I., OTTEWILL, R. H., LINDNER, P., OBERTHÜR, R. C. & RENNIE, A. R. 1990 Small angle neutron scattering studies on ordered polymer colloid dispersions. *Langmuir* **6**, 303–307.
- GOODWIN, J. W., HEARN, J., HO, C. C. & OTTEWILL, R. H. 1974 Studies on the preparation and characterization of monodisperse polystyrene latices. *Colloid Polym. Sci.* **252**, 464–471.
- HESS, O., LOOSE, W., WEIDER, T. & HESS, S. 1989 Shear-induced anisotropy of the structure of dense fluids. *Physica B* **156/157**, 505–507.
- HOFFMANN, R. L. 1972 Discontinuous and dilatant viscosity behaviour in concentrated suspensions. I. Observation of a flow instability. *Trans. Soc. Rheol.* **16**, 155–173.
- HOFFMANN, R. L. 1974 Discontinuous and dilatant viscosity behaviour in concentrated suspensions II. Theory and experimental tests. *J. Colloid Interface Sci.* **46**, 491–506.
- HOOVER, W. G. & REE, F. H. 1986 Melting transition and communal entropy for hard spheres. *J. Chem. Phys.* **49**, 3609–3617.
- VAN DEN HULL, H. J. & VANDERHOFF, J. W. 1970 Influences on the mechanism of emulsion polymerization of styrene from characterization of the polymer end-groups. *Br. Polym. J.* **2**, 121–127.
- ILL 1988 *Guide to Neutron Research Facilities at the Institut Laue-Langevin, Grenoble*. Institut Laue-Langevin, Grenoble.
- LINDNER, P. & OBERTHÜR, R. C. 1984 Apparatus for the investigation of liquid systems in a shear gradient by small angle neutron scattering (SANS). *Rev. Phys. Applic.* **19**, 759–763.
- LINDNER, P., MARKOVIĆ I., OBERTHÜR, R. C., OTTEWILL, R. H. & RENNIE, A. R. 1988 Small angle neutron scattering studies of polymer latices under sheared conditions. *Prog. Colloid Polym. Sci.* **76**, 47–50.
- LOOSE, W. & HESS, S. 1989 Rheology of dense model fluids in nonequilibrium molecular dynamics: shear thinning and ordering transition. *Rheol. Acta* **28**, 91–101.
- MARKOVIĆ, I., OTTEWILL, R. H., UNDERWOOD, S. M. & TADROS, TH. F. 1986 Investigations on concentrated nonaqueous polymer latices. *Langmuir* **2**, 625–630.
- VAN MEGEN, W., UNDERWOOD, S. M., OTTEWILL, R. H., WILLIAMS, N. ST. J. & PUSEY, P. N. 1987 Particle diffusion in concentrated dispersions. *Faraday Discuss. chem. Soc.* **83**, 47–57.
- OTTEWILL, R. H. 1987 Characterization of polymer colloids. In *Future Directions in Polymer Colloids* (Edited by EL-AASSER, & FITCH, R. M.), pp. 253–275. Nijhoff, Dordrecht.
- OTTEWILL, R. H. 1989 Colloid stability and instability: “order disorder”. *Langmuir* **5**, 4–11.
- OTTEWILL, R. H. & WILLIAMS, N. ST. J. 1987 Study of particle motion in concentrated dispersions by tracer diffusion. *Nature* **325**, 232–234 (1987).
- REINER, M. 1960 *Lectures on Theoretical Rheology*. North-Holland, Amsterdam.
- RENNIE, A. R., ASHDOWN, S., LINDNER, P., MARKOVIĆ I., OBERTHÜR, R. C. & OTTEWILL, R. H. 1990 Behaviour of polymer colloids under shear studied by small angle neutron scattering. In *Proc. NATO Advanced Study Institute on Polymer Colloids*, Strasbourg, pp. 453–462.

- RONIS, D. 1984 Theory of fluctuations in colloidal suspensions undergoing steady shear flow. *Phys. Rev.* **A29**, 1453–1460.
- RONIS, D. 1986 Configurational viscosity of dilute colloidal suspensions. *Phys. Rev.* **A34**, 1472–1480.
- SCHWARZL, J. F. & HESS, S. 1986 Shear-flow-induced distortion of the structure of a fluid: application of a simple kinetic equation. *Phys. Rev.* **A33**, 4277–4283.
- TOMITA, M. & VAN DE VEN, T. G. M. 1984 The structure of sheared ordered lattices. *J. Colloid Interface Sci.* **99**, 374–386.
- VAN DE VEN, T. G. M. 1988 Rheo-optics of dilute dispersions. *Mater. Sci. Forum* 25–26, 59–86.
- VAN DE VEN, T. G. M. 1990 Rheo- and electro-optics of colloidal dispersions. In *Proc. NATO Advanced Study Institute on Polymer Colloids*, Strasbourg, pp. 247–267.